

Possible surface magnetism in the topological Kondo insulator candidate FeSi

Yuhang Deng ^{1,*}, Yifei Yan ², Haozhe Wang ³, Eric Lee-Wong ⁴, Camilla M. Moir ¹,
Yuankan Fang ¹, Weiwei Xie ³ and M. Brian Maple ^{1,†}¹Department of Physics, University of California, San Diego, California 92093, USA²Department of Physics, University of Science and Technology of China, Hefei, Anhui 230026, China³Department of Chemistry, Michigan State University, East Lansing, Michigan 48824, USA⁴Department of NanoEngineering, University of California, San Diego, California 92093, USA

(Received 30 April 2023; accepted 11 September 2023; published 27 September 2023)

Our group has previously reported the existence of a conducting surface state (CSS) in FeSi, a candidate for a d -electron topological Kondo insulator (TKI), at low temperature. In this paper, we present the electrical transport properties of single crystals of FeSi studied in the phase space of temperature (T), magnetic field (B), and the angle (θ) between the electrical current and B . The normalized T -dependent electrical resistance (R) of a successively thinned FeSi crystal provides further confirmation of the existence of a CSS. We report that, in the CSS, the magnetoresistance (MR) exhibits a hysteresis loop bounded within ± 0.5 T, suggesting two-dimensional magnetic ordering. The hysteretic MR is asymmetric in B and anisotropic with respect to θ . Further exploration of $R(\theta)$ at a fixed field of 9 T reveals an initial progressive rotation of the axis for twofold rotational symmetry from 2 to 10 K, then a stabilized axis for twofold symmetry until, at $T > 40$ K, the anisotropy vanishes, coincident with the disappearance of the CSS. These observations point to a possible magnetically ordered surface state that has been reported in similar systems such as FeSi nanofilms and bulk SmB₆.

DOI: [10.1103/PhysRevB.108.115158](https://doi.org/10.1103/PhysRevB.108.115158)

I. INTRODUCTION

Since the 1960s, researchers have revealed many anomalous properties of the correlated d -electron compound FeSi, including a continuous transition with decreasing temperature from a metal with a localized magnetic moment to a semiconductor with a small gap ~ 60 meV and a nonmagnetic ground state [1–5]. Our group reported evidence for a conducting surface state (CSS) in FeSi in which the electrical resistance $R(T)$ exhibits metallic behavior with $dR/dT > 0$ below a maximum in $R(T)$ at $T_S \approx 19$ K that marks the onset of the CSS [6]. Subsequently, several papers reporting studies on FeSi single crystals have been published that support our claim of the existence of a CSS in FeSi, including a paper reporting a high-resolution tunneling spectroscopy study of the FeSi (110) surface [7] and a paper involving electrical transport measurements on a FeSi single crystal using a double-sided Corbino disk geometry [8]. Recently, Dzero *et al.* [9,10] proposed that a group of narrow-gap f -electron semiconductors referred to as Kondo insulators (KIs) could have CSSs of topological origin. This provided a possible explanation for the saturation of $R(T)$ of SmB₆ < 4 K to a constant value in terms of the formation of a topological CSS. In extensive experiments, during the past several years, researchers have established that SmB₆ has a CSS, with evidence that it is a topological KI (TKI) [11–14]. In our previous work [15], we noted that many of the properties of FeSi resemble those

of SmB₆ and suggested that the CSS could have a topological origin, and FeSi could be an example of a correlated d -electron TKI.

While many experimental and theoretical researchers have been focused on the anomalous magnetic susceptibility and metal-insulator transition at high temperatures of FeSi, Paschen *et al.* [16] conducted a comprehensive study of the electrical transport, thermal, and magnetic properties of FeSi down to very low temperatures. The Hall effect, magnetization, and electrical resistivity measurements on a very high-quality FeSi single crystal with a small Fe (Si) excess (deficiency) of up to 4% revealed evidence of a metallic state in FeSi with interacting magnetic moments < 1 K. Paschen *et al.* [16] attributed this metallic state to the formation of impurity bands out of ppm-level donor states. Hysteresis in magnetoresistance (MR) and an anomalous Hall effect were reported for SmB₆ below the onset temperature of its low-temperature resistivity plateau, leading the authors to propose the existence of a ferromagnetic, topologically nontrivial surface state with a quantized conductance value of e^2/h stemming from the chiral edge channels of ferromagnetic domain walls [17]. Considering the resemblance in behavior of the resistivity under magnetic fields between FeSi and SmB₆ and a report of a spin-orbit coupled ferromagnetic surface state originating from the Zak phase in FeSi nanofilms [18], we undertook a search for evidence of magnetic ordering in the CSS of FeSi single crystals. To affect this search, we carried out electrical resistance $R(T)$ measurements on rod-shaped FeSi single crystals previously studied in our lab [6,15] as a function of temperature (T), applied magnetic field (B), and angle (θ) of rotation of the FeSi single crystal about its long

*Corresponding author: yud001@physics.ucsd.edu

†Corresponding author: mbmaple@ucsd.edu

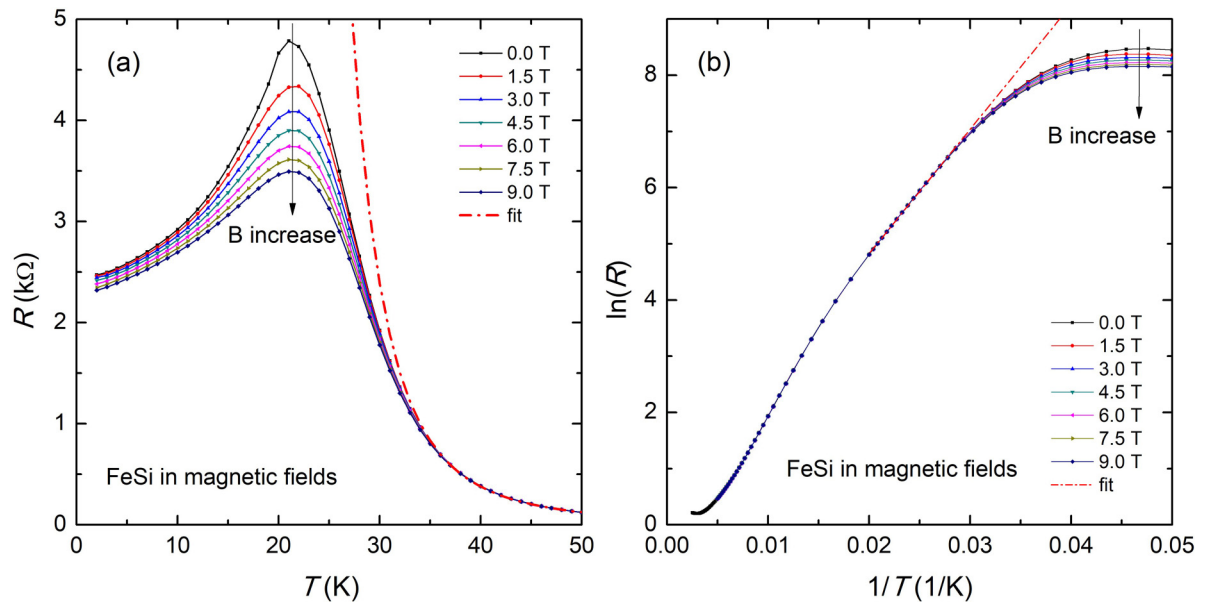


FIG. 1. Plots of (a) electrical resistance R vs temperature T and (b) $\ln(R)$ vs $1/T$ in magnetic fields B between 0 and 9 T for FeSi. The magnetoresistance (MR), defined as $MR \equiv \Delta R(B, T)/R(0, T) = [R(B, T) - R(0, T)]/R(0, T)$, is negative below ~ 34 K, and its magnitude is largest at ~ 21.5 K, where $R(B, T)$ exhibits a maximum. An extrapolation of the linear region between 34 and 50 K in (b) to lower temperatures (red dashed-dotted line) can be used to estimate the temperature of the onset of the surface state T_S .

axis, which is perpendicular to B and parallel to the electrical current (see diagram in Fig. 4(d)). Below the temperature of the peak in $R(T)$ of FeSi, we observed hysteresis in the MR of the sample as well as anisotropic behavior of the MR with respect to θ . Moreover, the axis of the anisotropic MR exhibits a gradual rotation as the temperature increases from 2 to 10 K. Our results suggest that some type of magnetic ordering is associated with the CSS of FeSi, which may be an example of two-dimensional (2D) magnetic order, possibly ferromagnetic, in a d -electron KI.

II. EXPERIMENTAL METHODS

A. Single-crystalline synthesis and x-ray diffraction measurements

High-quality FeSi single-crystalline samples were synthesized in a molten tin flux as described in Ref. [6]. Several single crystals were selected and examined in a Rigaku Synergy-S single-crystal x-ray diffractometer equipped with Mo radiation ($\lambda_{K\alpha} = 0.71073 \text{ \AA}$) to obtain the structure and crystal facet information. The crystal was measured with an exposure time of 10 s and a scanning 2θ width of 0.5° at room temperature. The data were processed in CrysAlis software, and structural refinement was conducted with the SHELXTL package using direct methods and refined by full-matrix least-squares on F^2 .

B. Electrical transport measurements

To establish a good surface to make electrical contact for transport measurements, samples were soaked in 20% HF aqueous solution for 10 min, after which platinum or gold leads were attached using silver paint or silver epoxy when mechanically strong electrical contacts were necessary. Elec-

trical resistance, $R(T, B, \theta)$, measurements in the ranges for T , B , and θ of $2 \text{ K} \leq T \leq 300 \text{ K}$, $0 \leq B \leq 9 \text{ T}$, and $0^\circ \leq \theta \leq 360^\circ$ were performed in a Quantum Design Physical Property Measurement System (PPMS) DynaCool with an electrical transport option and a horizontal rotator. A standard four-probe technique was used to measure the electrical resistance with a low frequency (0.4 or 0.5 Hz) ac current excitation of 0.1 mA at high temperature and 0.01 mA at low temperature.

III. RESULTS AND DISCUSSION

To obtain further insight into the structural features and crystal orientation information of FeSi grown from a Sn flux, several single crystals were investigated to extract elemental distributions and an accurate determination of interatomic distances and coordination environments. The detailed refinement and atomic coordinate information are presented in Tables S1 and S2 in the Supplemental Material [19]. All samples crystallize in the cubic chiral space group $P2_13$ (No. 198) with atoms located at two $4a$ sites. Upon careful examination of the two $4a$ sites, no Sn flux impurity was detected, and both sites are fully occupied by Fe and Si atoms, respectively, based on the chemical composition refinement. Single-crystal x-ray diffraction measurements were also conducted to determine the crystal directions. Accordingly, the Sn flux as-grown rod-shaped FeSi crystals were found to grow along the face diagonal $\langle 011 \rangle$ direction.

The electrical resistance $R(T)$ of a rod-shaped FeSi single crystal with a length of ~ 2.4 mm and a thickness of $\sim 40 \mu\text{m}$ grown along its $[0\bar{1}1]$ direction was measured as a function of temperature in magnetic fields oriented perpendicular to the electrical current (also along $[0\bar{1}1]$) up to 9 T. As shown

in Fig. 1, the resistance of the sample is independent of the magnetic field between room temperature and 34 K. However, <34 K, the resistance decreases with magnetic field, implying a negative MR defined by $MR \equiv \Delta R(B, T)/R(0, T) = [R(B, T) - R(0, T)]/R(0, T)$. At ambient pressure, from 160 to 34 K, the $R(T)$ curve of FeSi can be described well by an Arrhenius law in two different temperature ranges (160–70 and 55–35 K) [6,15]. Below 34 K, this two-gap semiconductor model fails to describe the behavior of $R(T)$ which features a peak at ~ 21.5 K, indicating a crossover from semiconducting to metallic behavior. The behavior of $R(T)$ in magnetic fields suggests that the bulk insulating state of FeSi is hardly affected by fields up to 9 T, whereas the conductivity of the CSS is enhanced by a magnetic field. The CSS electrically shorts the bulk state significantly, as indicated by the much lower measured resistance than extrapolations of the resistance >34 K fitted with the second energy gap activation model in Fig. 1 (red dashed-dotted lines). As a result, the negative transverse MR must be from the CSS of FeSi.

Many metals show a positive MR. By using a simple two-band model [20], the transverse MR of metals with a closed Fermi surface should show a quadratic magnetic field dependence ($MR \sim B^2$) at low field and saturate in the high-field limit, whereas for metals with an open Fermi surface in certain crystallographic directions, the MR would maintain its B^2 dependence without saturation even at high fields. This rough model has successfully explained the MR of some nonmagnetic simple metals (e.g., copper, silver, and gold) and has been used to provide information about the topology of the Fermi surface of metals [21]. However, the two-band model has a problem with explaining the linear MR in some alkali metals such as potassium which is usually thought to have a closed and nearly spherical Fermi surface but instead exhibits a linear, unsaturated MR, up to 5.5 T [22]. Moreover, the two-band model is insufficient in explaining the MR in metals with magnetic moments, such as Fe which has a negative and hysteretic transverse MR along some crystal axes at low temperatures [23] or Dy and Ho which have complicated MR depending on temperature, strength, and directions of applied fields [24].

Considering the inability of the two-band model to account for the MR of magnetic materials, we briefly describe the MR of some KIs which are believed to have a topological surface state at low temperatures to give an overall perspective of how the MR of potential TKIs would typically behave if a general rule existed.

SmB₆: As a prototype TKI, SmB₆ shows a crossover from a slightly positive MR just above its onset temperature (5 K) of its putative topological metallic surface state, to a pronounced negative MR with decreasing temperature [25]. For even lower temperatures, Chen *et al.* [25] reported a small positive MR at 2 K, while Nakajima *et al.* [17] observed a small negative MR < 1 K. In both studies, the resistance measurements were made with the current in the (100) plane and a perpendicular field.

YbB₁₂: The high-temperature KI region shows a negative transverse MR suggesting a field-induced closing of the hybridization gap. The MR is large and negative at 2.5 K and 14 T, and its magnitude decreases upon cooling < 2.5 K,

where the metallic surface emerges as signaled by the resistivity plateau [26].

FeSb₂: It was recently suggested by angle-resolved photoemission spectroscopy that a metallic surface state exists in FeSb₂, another *d*-electron KI candidate. At 4.2 K, FeSb₂ has a positive MR that persists up to 17.5 T [27]. However, at 3 K, below the onset of the temperature at which the resistance saturates, the MR is first negative and then becomes positive > 1.5 T [28]. This negative MR was explained within the framework of weak electronic localization in an extrinsic semiconductor with ppm-level impurities [28]. However, we note that the negative MR of the FeSi single crystal studied herein has its largest magnitude at ~ 21.5 K, where $R(B, T)$ exhibits a maximum, qualitatively like what was found in SmB₆ and YbB₁₂, and is found in the region of temperature where the normalized resistance is sensitive to the change in cross-sectional area of the rod-shaped FeSi single crystal (see Fig. S1 in the Supplemental Material [19]). Based on these observations, we conclude that the negative MR is unlikely associated with the formation of an extrinsic impurity conduction band, and it cannot be accounted for in terms of an ordinary two-band model for simple metals.

To further understand the effect of magnetic fields on the CSS, the field dependence of the resistance of the same sample was measured with the sample positioned at fixed angles (θ) about its long axis $[0\bar{1}1]$. A magnetic field perpendicular to $[0\bar{1}1]$ was swept from 4 to -4 T then back to 4 T to determine whether the resistance depends on the history of the applied field. The results are shown for measurements made at 2 and 10 K in Fig. 2 and 20 and 30 K in Fig. 3. The $R(B_{\perp[0\bar{1}1]})$ curves at these temperatures are anisotropic; the curves vary at different values of θ . Although the anisotropy persists from 2 to 30 K, the $R(B_{\perp[0\bar{1}1]})$ curves exhibit dramatically different types of behavior, regarding whether they are hysteretic and symmetric about $B = 0$ T, that depends on the history of the applied magnetic field and temperature. At 2 K [see Figs. 2(a) and 2(c)] and 10 K [see Figs. 2(b) and 2(d)], at fixed values of θ , the $R(B_{\perp[0\bar{1}1]})$ curves are asymmetric and exhibit hysteretic behavior in the region $-0.5 \text{ T} \leq B_{\perp[0\bar{1}1]} \leq 0.5 \text{ T}$ for changes in the sign of the magnetic field $B_{\perp[0\bar{1}1]}$. There is a switch of chirality of the hysteresis between 60° and 90° , the origin of which still needs further investigation but is apparently associated with the asymmetry of the MR. At 0° and 30° , the resistance for $B > 0$ is higher than that for $B < 0$, which corresponds to counterclockwise chirality. At 90° , 120° , and 150° , the resistance of $B < 0$ is higher than that for $B > 0$, and the chirality is clockwise. At 60° , the area of the hysteresis loop reaches its minimum accompanied with the suppression of the asymmetric MR. The results shown in Figs. 3(a) and 3(c) (20 K) and Figs. 3(b) and 3(d) (30 K), near or above the temperature at which $R(T)$ exhibits a peak, reveal that, in contrast to the behavior of the $R(B_{\perp[0\bar{1}1]})$ curves in Fig. 2, the $R(B_{\perp[0\bar{1}1]})$ curves are now symmetric with respect to the sign of the magnetic field $B_{\perp[0\bar{1}1]}$, and the hysteresis in the MR is no longer present.

The asymmetric and hysteretic behavior observed in the $R(B_{\perp[0\bar{1}1]})$ curves at fixed angles of θ shown in Fig. 2 for temperatures of 2 and 10 K suggest the possible formation of 2D ferromagnetic order associated with the CSS state in FeSi. Evidence for ferromagnetic order near T_S has also been

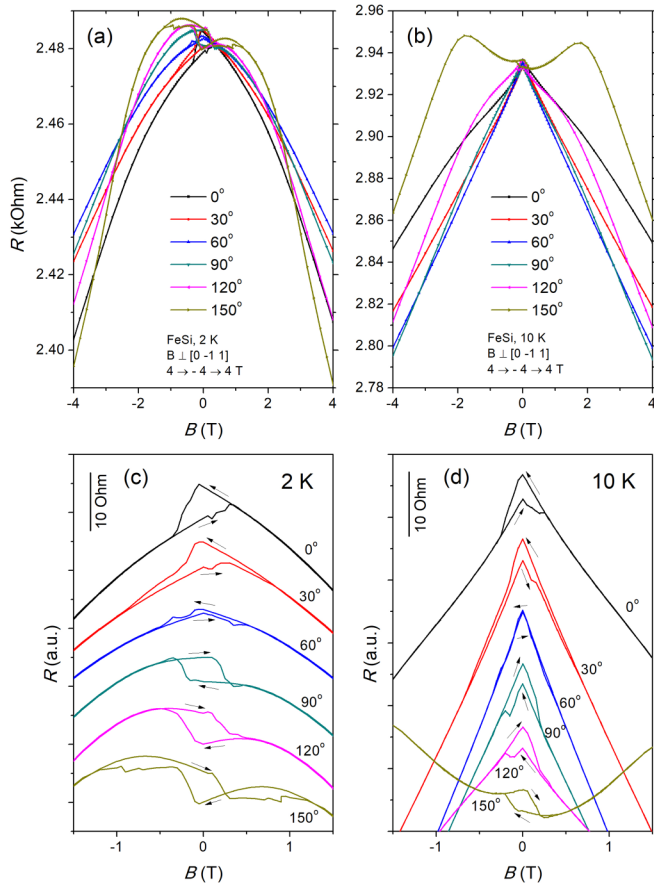


FIG. 2. Electrical resistance R vs magnetic field $B_{\perp[0\bar{1}1]}$ for various values of the angle θ at 2 and 10 K, where $B_{\perp[0\bar{1}1]}$ is perpendicular to the axis $[0\bar{1}1]$ of the rod-shaped FeSi single crystal, and at various values of the angle θ about the FeSi crystal axis. Plots of R vs $B_{\perp[0\bar{1}1]}$ are shown for (a) and (b) $-4 \text{ T} \leq B_{\perp[0\bar{1}1]} \leq 4 \text{ T}$ and (c) and (d) $-1 \text{ T} \leq B_{\perp[0\bar{1}1]} \leq 1 \text{ T}$, where the $R(B_{\perp[0\bar{1}1]})$ curves are shifted vertically for visual clarity. Arrows point to the direction of the magnetoresistance (MR) loops. Note the switch in chirality of the hysteresis between 60° and 90° .

suggested based on magnetic field-modulated microwave spectroscopy measurements reported by Breindel *et al.* [15]. Similar hysteretic behavior as a function of magnetic field has been observed in Hall effect studies of chemical-vapor-transport-grown single crystals of FeSi by Paschen *et al.* [16] and suggested to be due to some type of magnetic order or interaction between magnetic moments [16]. Recently, Hall effect measurements on the (111) surface of thin films of FeSi grown on silicon substrates were observed to exhibit hysteretic behavior as a function of B in the region $<1 \text{ T}$, which was attributed to ferromagnetic order in a CSS. The ferromagnetic order was confirmed by magnetization measurements and polarized neutron reflectometry on these FeSi films with thicknesses of the order of 10 nm [18]. Interestingly, hysteresis in MR measurements performed on SmB₆ single crystals have been interpreted in terms of ferromagnetic ordering of electrons in the CSS of a TKI [17].

Displayed in Fig. 4 are isothermal polar plots of the normalized angular-dependent MR (AMR) patterns at 9 T, $\text{AMR} \equiv 100 \times [R(\theta) - R(-14^\circ)]/R(-14^\circ)$ (%) at various

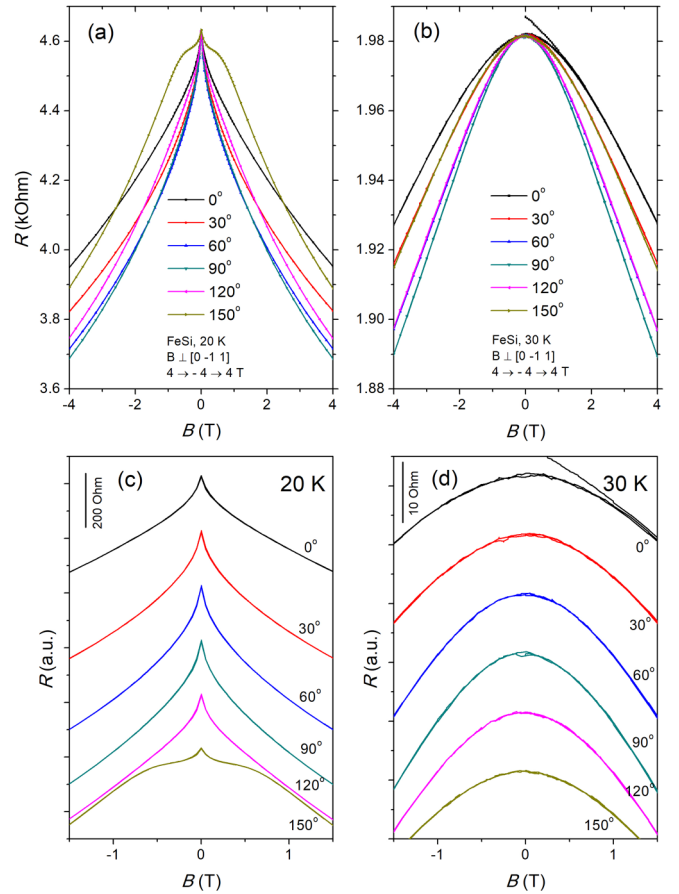


FIG. 3. Electrical resistance R vs magnetic field $B_{\perp[0\bar{1}1]}$ for various values of the angle θ at 20 and 30 K, where $B_{\perp[0\bar{1}1]}$ is perpendicular to the axis $[0\bar{1}1]$ of the rod-shaped FeSi single crystal, and at various values of the angle θ about the FeSi crystal axis. Plots of R vs $B_{\perp[0\bar{1}1]}$ are shown for (a) and (b) $-4 \text{ T} \leq B_{\perp[0\bar{1}1]} \leq 4 \text{ T}$ and (c) and (d) $-1 \text{ T} \leq B_{\perp[0\bar{1}1]} \leq 1 \text{ T}$, where curves are shifted vertically for visual clarity.

temperatures indicated in panels (a)–(c) for $B_{\perp[0\bar{1}1]}$, where the long axis of the rod-shaped FeSi crystal is in the $[0\bar{1}1]$ direction. A diagram in Fig. 4(d) shows the placement of current I and voltage V electrodes on the rod-shaped FeSi single crystal (blue color) and the magnetic field B direction which was aligned perpendicular to the axis of the FeSi crystal and oriented at an angle of rotation θ about the crystal axis. In addition, the crystal axis and I were arranged along the $[0\bar{1}1]$ direction. In panel (a), the polar plots have a nearly symmetrical peanut shape in which the long axis rotates in the clockwise direction by $\sim 60^\circ$ from 2 to 10 K; in panel (b), the polar plots evolve from a peanut shape to a circular shape from 20 to 40 K, and the axis does not rotate; while in panel (c), the polar plots are circular with an amplitude that decreases with increasing temperature from 50 to 80 K. The twofold rotational (C_2) symmetry was also observed in SmB₆ plate-shaped [25] and rod-shaped [29] samples, and a FeSb₂ plate-shaped [30] sample when MR was measured below the temperature of the onset of their resistivity plateaus, which was thought to originate from the surface conductivity of these two putative TKIs. The crossover from C_4 symmetry to C_2 symmetry in the cubic SmB₆ can be interpreted because of a

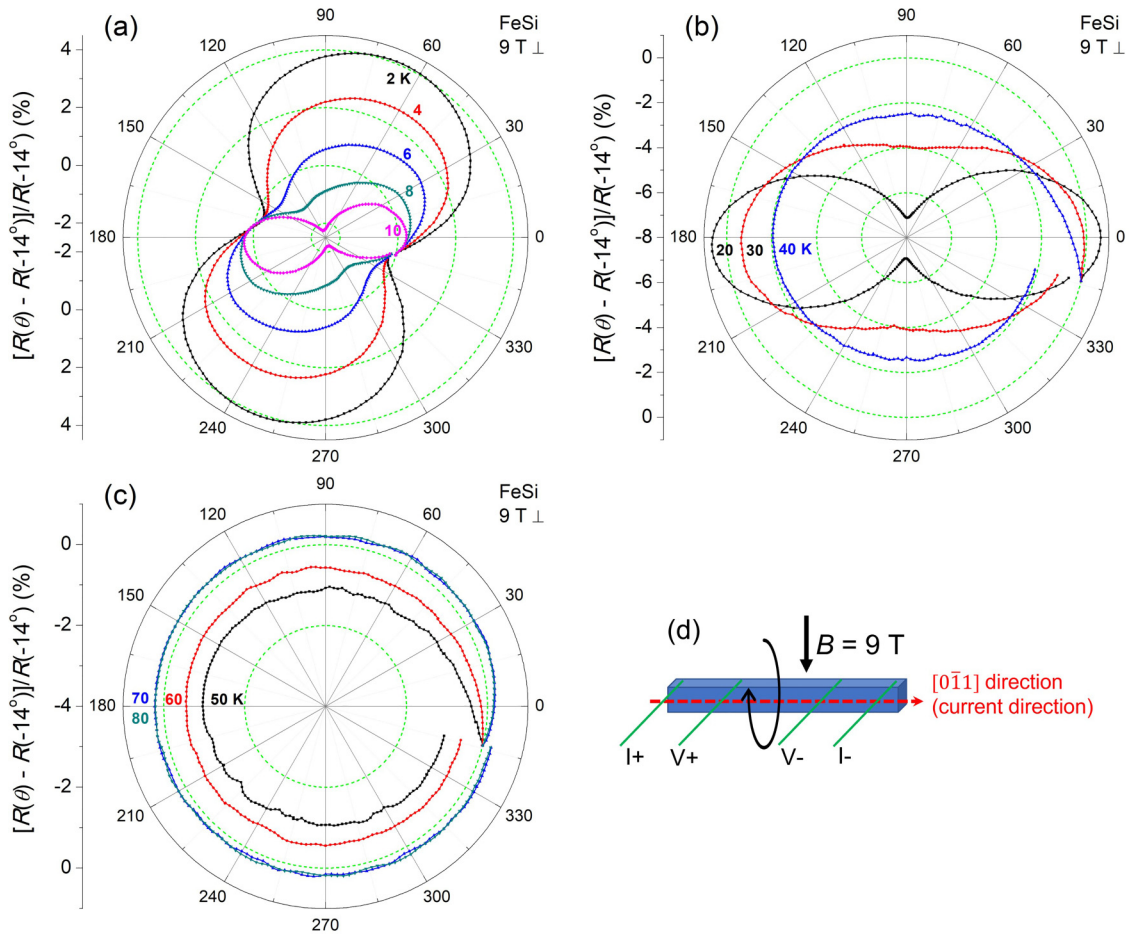


FIG. 4. Isothermal polar plots of the normalized angular-dependent magnetoresistance (AMR) at 9 T, $\text{AMR} \equiv 100 \times [R(\theta) - R(-14^\circ)]/R(-14^\circ)$ (%) at various temperatures indicated in the three panels for $B_{\perp[0\bar{1}1]}$, where the axis of the rod-shaped FeSi crystal is in the $[0\bar{1}1]$ direction: (a) $T = 2, 4, 6, 8,$ and 10 K; (b) $T = 20, 30,$ and 40 K; and (c) $T = 50, 60, 70,$ and 80 K. (d) Schematic diagram showing the rod-shaped FeSi single crystal (blue color), the disposition of current I and voltage V electrodes, the magnetic field B which is perpendicular to the axis of the rod-shaped FeSi crystal and oriented at an angle θ of rotation about the crystal axis. The small mismatches at the beginning and end of some curves are due to initial temperature control instability of the PPMS DynaCool in which the measurements were made.

rotational symmetry-breaking nematic ordering on the surface of a TKI [31]. More strikingly, the peanut-shaped AMR of SmB_6 and FeSb_2 [30] rotates with temperature where surface conductivity dominates, remarkably like the phenomenon observed here for FeSi.

Shown in Fig. 5 is the degree of anisotropy $A_n \equiv (R_{\max} - R_{\min})/R_{\max}$ vs T between 0 and 50 K, where R_{\max} and R_{\min} are the maximum and minimum values of R , respectively, of the isothermal MR at 9 T. A clear correspondence exists between the types of patterns of the AMR and the CSS with or without hysteresis in the MR. Below T_s (2–15 K), the MR in the FeSi CSS shows a hysteresis loop (see Fig. 2), corresponding to a peanut-shaped AMR with a temperature-dependent change in the direction of the long axis seen in Fig. 4(a). Between 20 and ~ 40 K, the CSS is still present, but the hysteresis in the MR disappears (see Fig. 3) accompanied by a stabilized yet less anisotropic AMR shown in Fig. 4(b). At even higher temperatures where the insulating state dominates, the MR of FeSi becomes negligible (see Fig. 1) and thus is isotropic, as shown in Fig. 4(c).

A possible source of hysteresis in the MR of FeSi is the occurrence of ferromagnetic order. In ferromagnetic materials, the MR depends on the orientation of the magnetization with respect to the direction of the electrical current. The hysteretic and anisotropic MR found in FeSi could be due to magnetic ordering, possibly ferromagnetic, associated with the CSS. As discussed above, similar phenomena were observed in a SmB_6 slab [17] and FeSi nanofilms [18], both of which were attributed to the presence of a ferromagnetic metallic surface state. The origin of this state, however, has been interpreted in different ways in different systems. Ohtsuka *et al.* [18] did not classify FeSi as a topological insulator and instead attributed the CSS to a Zak phase, a Berry phase accumulated by a Bloch state along a path across the Brillouin zone, based on various measurements they performed on FeSi and first-principles calculations. However, a Kondo breakdown scenario [32] provides another possible explanation for the formation of the magnetic CSS in FeSi in terms of a TKI. At the surface of a TKI, the local magnetic moments cannot be fully screened by conduction electrons. This Kondo breakdown liberates

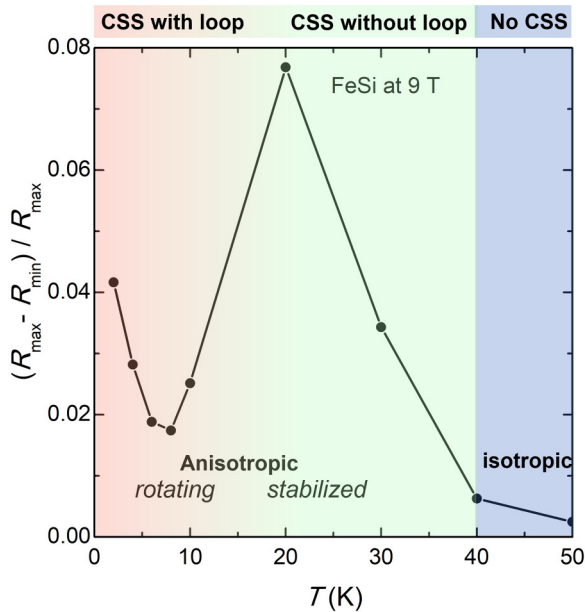


FIG. 5. Degree of anisotropy $An \equiv (R_{\max} - R_{\min})/R_{\max}$, where R_{\max} and R_{\min} are the maximum and minimum values of R , respectively, of the isothermal magnetoresistance at 9 T, vs temperature T between 0 and 50 K. Regions of anisotropic (rotating or stabilized) and isotropic behavior are indicated in the colored regions of the figure.

unquenched magnetic moments and many carriers that would otherwise be confined inside Kondo singlets at the surface, leading to protection of the surface state against decreasing thickness. Moreover, a chiral Kondo lattice will form due to the surface Kondo breakdown, with a ground state that is either magnetically ordered or a heavy Fermi liquid [32]. This theory was supported by the discovery of a hysteretic MR in SmB_6 nanowires [33]. Compared with bulk samples, SmB_6 nanowires (tens of nanometers) showed even higher resistivity plateau temperatures, which is quite unusual because perfect topological protection of the surface states requires an infinite bulk. With the possibility of surface Kondo breakdown, the topological surface in SmB_6 was predicted to be persistent even in an ultrathin film with thickness of ~ 10 nm [32]. He *et al.* [33] also found the anomalous MR hysteresis only appeared < 8 K, less obvious with increasing temperature and increasing thickness of the nanowires. Based on the Mermin-Wagner theorem, reduced dimensionality tends to destroy long-range magnetic ordering in conventional ferromagnetic materials. Kondo breakdown, resilient in small dimensions, involving weaker Kondo screening and a stronger RKKY interaction at the surface, seems more likely the origin of the magnetic ordering in SmB_6 nanowires.

In an early study of flux grown single crystals of FeSi, Paschen *et al.* [16] observed a resistivity plateau < 1 K, accompanied by hysteresis in the Hall voltage, although no information was provided about the dimensions of the FeSi single crystals on which the measurements were made. In this paper, electrical resistivity measurements were made on rod-shaped FeSi single crystals with thicknesses of ~ 50 μm . The measurements revealed a decrease in $R(T)$ with decreasing

temperature below ~ 21 K and hysteresis in the anisotropic MR AMR. Ohtsuka *et al.* [18] synthesized FeSi nanofilms on Si (111) substrates, with thicknesses varying from 5 to 60 nm along the [111] direction. At temperatures < 100 K, the Hall conductivity (σ_{xy}) and normalized magnetization M vs magnetic field B curves were found to display clear hysteresis loops whose magnitudes depend inversely on the thickness of the nanofilms. The area of the hysteresis loop in σ_{xy} decreases with increasing thickness [18], as found previously in the MR of SmB_6 nanowires [33]. There is a report on FeSi nanowires showing magnetization hysteresis even at room temperature, although the authors attributed this to the interaction between charge carriers and localized dangling bond spins which is significant at the nanoscale [34]. We could not exclude the possibility that the observed hysteresis in AMR associated with the CSS of FeSi arises from magnetic ordering formed by an impurity conduction band or dangling covalent bonds terminated at the surface. However, the inverse correlation of the MR/magnetization hysteresis loop size with the sample dimensions observed in different literature reports suggests the Kondo breakdown picture may be the origin of the magnetic order in the CSS of FeSi.

IV. CONCLUDING REMARKS

Transverse MR measurements at low temperatures were conducted on high-quality FeSi single crystals which grow in the direction of the face diagonal of the cubic B20 structure, $[0\bar{1}1]$. A negative MR was observed below the onset temperature T_S of the CSS, in contrast to the positive MR often seen in simple metals, revealing an unusual mechanism of charge transport in the metallic surface state of FeSi. Moreover, anisotropic hysteresis in the MR was observed in the CSS, resembling what has been reported for SmB_6 , the prototype f -electron KI to which FeSi is being compared, pointing to possible surface magnetic ordering. The relationship between electrical resistance of FeSi and the angle θ of the magnetic field at $B = 9$ T, $R(\theta, 9$ T), was measured at various fixed temperatures. The twofold rotational symmetry of $R(\theta, 9$ T) that was observed may reflect the emergence of the CSS of FeSi. However, the underlying reason for the rotation of the peanut-shaped AMR is not clear and awaits further investigation.

Two theoretical scenarios, the Zak phase and Kondo breakdown, were discussed herein as possible explanations for the surface magnetic ordering indicated by the hysteresis in the MR of FeSi. We note that the intriguing phenomena found in FeSi could be attributed to Kondo breakdown on the surface, which can create unscreened magnetic moments and liberate unbound conduction electrons from Kondo singlets, thus introducing a metallic, magnetically ordered surface. We expect the Kondo breakdown and its effects on the surface conduction and magnetism would be more dominant in the TKI with smaller dimensions or larger surface-to-volume ratios, which is consistent with our studies and other reports by Paschen *et al.* [16], Ohtsuka *et al.* [18], and Hung *et al.* [34]. To further test the Kondo breakdown scenario in FeSi, we plan to perform MR, Hall effect, and magnetization measurements on a successively thinned rod-shaped sample or powdered samples to examine whether hysteresis in samples with larger

surface areas will be more pronounced. Sensitive and spatially resolved magnetization mapping characterizations such as magnetic force microscopy, magneto-optic Kerr microscopy, and optically detected magnetic resonance of diamond nitrogen-vacancy centers would be extremely useful to image any possible magnetization structures of the CSS of FeSi.

ACKNOWLEDGMENTS

Research at University of California, San Diego, was supported by the National Nuclear Security Administration under the Stewardship Science Academic Alliance Program

through the U.S. Department of Energy (DOE) under Grant No. DE-NA0004086 (electrical transport measurements) and the U.S. DOE Basic Energy Sciences (BES) under Grant No. DE-FG02-04ER46105 (single-crystal growth and characterization). This paper was sponsored in part by the UC San Diego Materials Research Science and Engineering Center (UCSD MRSEC), supported by the National Science Foundation (Grant No. DMR-2011924). Research at Michigan State University was supported by the U.S. DOE-BES under Contract No. DE-SC0023648 (single-crystal x-ray diffraction). It is a pleasure to acknowledge informative discussions with Professor Peter Riseborough.

-
- [1] H. Watanabe, H. Yamamoto, and K. I. Ito, Neutron diffraction study of the intermetallic compound FeSi, *J. Phys. Soc. Jpn.* **18**, 995 (1963).
- [2] V. Jaccarino, G. K. Wertheim, J. K. Wernick, L. R. Walker, and S. Araj, Paramagnetic excited state of FeSi, *Phys. Rev.* **160**, 476 (1967).
- [3] Z. Schlesinger, Z. Fisk, H. Zhang, M. B. Maple, J. F. DiTusa, and G. Aeppli, Unconventional Charge Gap Formation in FeSi, *Phys. Rev. Lett.* **71**, 1748 (1993).
- [4] B. C. Sales, E. C. Jones, B. C. Chakoumakos, J. A. Fernandez-Baca, H. E. Harmon, J. W. Sharp, and E. H. Völckmann, Magnetic, transport, and structural properties of $\text{Fe}_{1-x}\text{Ir}_x\text{Si}$, *Phys. Rev. B* **50**, 8207 (1994).
- [5] D. Mandrus, J. L. Sarrao, A. Migliori, J. D. Thompson, and Z. Fisk, Thermodynamics of FeSi, *Phys. Rev. B* **51**, 4763 (1995).
- [6] Y. Fang, S. Ran, W. Xie, S. Wang, Y. S. Meng, and M. Brian Maple, Evidence for a conducting surface ground state in high quality single crystalline FeSi, *Proc. Natl. Acad. Sci. USA* **115**, 8558 (2018).
- [7] B. Yang, M. Uphoff, Y. Zhang, J. Reichert, A. P. Seitsonen, A. Bauera, C. Pfleiderer, and J. V. Barth, Atomistic investigation of surface characteristics and electronic features at high-purity FeSi (110) presenting interfacial metallicity, *Proc. Natl. Acad. Sci. USA* **118**, e2021203118 (2021).
- [8] Y. S. Eo, K. Avers, J. A. Horn, H. Yoon, S. Saha, A. Suarez, M. S. Fuhrer, and J. Paglione, Extraordinary bulk-insulating behavior in the strongly correlated materials FeSi and FeSb_2 , *Appl. Phys. Lett.* **122**, 233102 (2023).
- [9] M. Dzero, K. Sun, V. Galitski, and P. Coleman, Topological Kondo Insulators, *Phys. Rev. Lett.* **104**, 106408 (2010).
- [10] M. Dzero, J. Xia, V. Galitski, and P. Coleman, Topological Kondo insulators, *Annu. Rev. Condens. Matter Phys.* **7**, 249 (2016).
- [11] M. Neupane, N. Alidoust, S.-Y. Xu, T. Kondo, Y. Ishida, D. J. Kim, C. Liu, I. Belopolski, Y. J. Jo, T.-R. Chang *et al.*, Surface electronic structure of the topological Kondo-insulator candidate correlated electron system SmB_6 , *Nat. Commun.* **4**, 2991 (2013).
- [12] J. Jiang, S. Li, T. Zhang, Z. Sun, F. Chen, Z. R. Ye, M. Xu, Q. Q. Ge, S. Y. Tan, X. H. Niu *et al.*, Observation of possible topological in-gap surface states in the Kondo insulator SmB_6 by photoemission, *Nat. Commun.* **4**, 3010 (2013).
- [13] N. Xu, P. K. Biswas, J. H. Dil, R. S. Dhaka, G. Landolt, S. Muff, C. E. Matt, X. Shi, N. C. Plumb, M. Radovic *et al.*, Direct observation of the spin texture in SmB_6 as evidence of the topological Kondo insulator, *Nat. Commun.* **5**, 4566 (2014).
- [14] G. Li, Z. Xiang, F. Yu, T. Asaba, B. Lawson, P. Cai, C. Tinsman, A. Berkley, S. Wolgast, Y. S. Eo *et al.*, Two-dimensional Fermi surfaces in Kondo insulator SmB_6 , *Science* **346**, 1208 (2014).
- [15] A. Breindel, Y. Deng, C. M. Moir, Y. Fang, S. Ran, H. Lou, S. Li, Q. Zeng, L. Shu, C. T. Wolowiec *et al.*, Probing FeSi, a *d*-electron topological Kondo insulator candidate, with magnetic field, pressure, and microwaves, *Proc. Natl. Acad. Sci. USA* **120**, e2216367120 (2023).
- [16] S. Paschen, E. Felder, M. A. Chernikov, L. Degiorgi, H. Schwer, H. R. Ott, D. P. Young, J. L. Sarrao, and Z. Fisk, Low-temperature transport, thermodynamic, and optical properties of FeSi, *Phys. Rev. B* **56**, 12916 (1997).
- [17] Y. Nakajima, P. Syers, X. Wang, R. Wang, and J. Paglione, One-dimensional edge state transport in a topological Kondo insulator, *Nat. Phys.* **12**, 213 (2016).
- [18] Y. Ohtsuka, N. Kanazawa, M. Hirayama, A. Matsui, T. Nomoto, R. Arita, T. Nakajima, T. Hanashima, V. Ukleev, H. Aoki *et al.*, Emergence of spin-orbit coupled ferromagnetic surface state derived from Zak phase in a nonmagnetic insulator FeSi, *Sci. Adv.* **7**, eabj0498 (2021).
- [19] See Supplemental Material at <http://link.aps.org/supplemental/10.1103/PhysRevB.108.115158> for the single-crystal structure refinement for FeSi; atomic coordinates and equivalent isotropic displacement parameters; and resistance vs temperature curves of a FeSi sample before and after being thinned.
- [20] I. M. Lifshitz, M. I. Azbel, and M. I. Kaganov, On the theory of galvanomagnetic effects in metals, *Sov. Phys. JETP* **3**, 143 (1956).
- [21] M. G. Priestley, Magnetoresistance of copper, silver and gold, *Philos. Mag.* **5**, 111 (1960).
- [22] P. A. Penz and R. Bowers, Transverse magnetoresistance of single crystals of potassium, *Solid State Commun.* **5**, 341 (1967).
- [23] A. Işin and R. V. Coleman, Temperature dependence of magnetoresistance in iron, *Phys. Rev.* **142**, 372 (1966).
- [24] A. R. Mackintosh and L. E. Spinel, Magnetoresistance in rare earth single crystals, *Solid State Commun.* **2**, 383 (1964).
- [25] F. Chen, C. Shang, Z. Jin, D. Zhao, Y. P. Wu, Z. J. Xiang, Z. C. Xia, A. F. Wang, X. G. Luo, T. Wu *et al.*, Magnetoresistance evidence of a surface state and a field dependent insulating state in the Kondo insulator SmB_6 , *Phys. Rev. B* **91**, 205133 (2015).

- [26] Z. Xiang, K. Chen, L. Chen, T. Asaba, Y. Sato, N. Zhang, D. Zhang, Y. Kasahara, F. Iga, W. A. Coniglio *et al.*, Hall Anomaly, Quantum Oscillations and Possible Lifshitz Transitions in Kondo Insulator YbB_{12} : Evidence for Unconventional Charge Transport, *Phys. Rev. X* **12**, 021050 (2022).
- [27] K. Xu, S. Chen, Y. He, J. He, S. Tang, C. Jia, E. Y. Ma, S. Mo, D. Lu, M. Hashimoto *et al.*, Metallic surface states in a correlated d -electron topological Kondo insulator candidate FeSb_2 , *Proc. Natl. Acad. Sci. USA* **117**, 15409 (2020).
- [28] H. Takahashi, R. Okazaki, Y. Yasui, and I. Terasaki, Low-temperature magnetotransport of the narrow-gap semiconductor FeSb_2 , *Phys. Rev. B* **84**, 205215 (2011).
- [29] Z. Yue, X. Wang, D. Wang, J. Wang, D. Culcer, and S. Dou, Crossover of magnetoresistance from fourfold to twofold symmetry in SmB_6 single crystal, a topological Kondo insulator, *J. Phys. Soc. Jpn.* **84**, 044717 (2015).
- [30] A. G. Eaton, FeSb_2 : A Riddle, Inside an Insulator, Wrapped in a Metal, Ph.D. dissertation, University of Cambridge, 2022.
- [31] B. Roy, J. Hofmann, V. Stanev, J. D. Sau, and V. Galitski, Excitonic and nematic instabilities on the surface of topological Kondo insulators, *Phys. Rev. B* **92**, 245431 (2015).
- [32] V. Alexandrov, P. Coleman, and O. Erten, Kondo Breakdown in Topological Kondo Insulators, *Phys. Rev. Lett.* **114**, 177202 (2015).
- [33] X. He, H. Gan, Z. Du, B. Ye, L. Zhou, Y. Tian, S. Deng, G. Guo, H. Lu, F. Liu *et al.*, Magnetoresistance anomaly in topological Kondo insulator SmB_6 nanowires with strong surface magnetism, *Adv. Sci.* **5**, 1700753 (2018).
- [34] S. Hung, T. T. Wang, L. Chu, and L. Chen, Orientation-dependent room-temperature ferromagnetism of FeSi nanowires and applications in nonvolatile memory devices, *J. Phys. Chem. C* **115**, 15592 (2011).